Available online at www.sciencedirect.com
SCIENCE DIRECT®
Thermochimica Acta 421 (2004) 141–149
thermochimica acta
www.elsevier.com/locate/tca

Mechanism of decomposition of manganese(II) oxalate dihydrate and manganese(II) oxalate trihydrate

B. Donkova [a,*], D. Mehandjiev [b,1]

[a] *Department of Inorganic Chemistry, Faculty of Chemistry, University of Sofia, 1 J. Bourchier Av., Sofia 1164, Bulgaria*
[b] *Institute of General and Inorganic Chemistry, Bulgarian Academy of Sciences, Acad. G. Bonchev Str. Bl. 11, Sofia 1113, Bulgaria*

Received 20 October 2003; received in revised form 27 March 2004; accepted 1 April 2004
Available online 24 May 2004

Abstract

The thermal behavior and magnetic properties of two manganese(II) oxalates crystallohydrates are studied and compared. $MnC_2O_4{\cdot}2H_2O$ crystallizes in monoclinic syngony, while the $MnC_2O_4{\cdot}3H_2O$—in orthorhombic. The difference in the crystal lattice is responsible for the different thermal behavior of the samples. This fact is proved by in situ measurement of the magnetic properties, TGA, DTA, DSC, and X-ray diffraction. The dehydration proceeds in one step with $MnC_2O_4{\cdot}2H_2O$ ($\Delta H = 86$ kJ/mol) and in three steps with $MnC_2O_4{\cdot}3H_2O$ ($\Delta H = 132$ kJ/mol). The exchange interaction between the manganese ions in $MnC_2O_4{\cdot}3H_2O$ is changing from antiferromagnetic to ferromagnetic during the entire dehydration process, while in the case of $MnC_2O_4{\cdot}2H_2O$ the same interaction remains almost constantly antiferromagnetic. The two crystallohydrates reveal different initial and final temperatures of dehydration, thus changing the region where the anhydrous oxalate exists. The oxidative decomposition of the anhydrous oxalate leads not only to Mn(III) but also to Mn(IV) and an oxidation process is much weaker when starting from $MnC_2O_4{\cdot}3H_2O$. This fact shows that the orthorhombic crystal lattice stabilizes the lower oxidation states of manganese. The annealing of the monoclinic $MnC_2O_4{\cdot}2H_2O$ at 450 °C leads to its complete transformation into Mn_3O_4 with hausmanite structure. At the same temperature, the orthorhombic $MnC_2O_4{\cdot}3H_2O$ gives not only Mn_3O_4 but also a great quantity of cubic Mn_2O_3.

Keywords: Magnetic properties; Decomposition; Synthesis; Manganese(II) oxalates

1. Introduction

The investigation of the processes of thermal decomposition in oxalate systems is related to their wide application as precursors for the preparation of nano-materials, superconductors, sorbents and catalysts. For this reason, the detailed knowledge of the oxidation states of the element under consideration is important.

The objects of the present study are the crystal hydrates in the system manganese(II) oxalate–water. It has been established that two crystal hydrates are formed in this system—$MnC_2O_4{\cdot}2H_2O$ and $MnC_2O_4{\cdot}3H_2O$ [1,2]. Both crystal hydrates differ in color and structure. The white α-$MnC_2O_4{\cdot}2H_2O$ is monoclinic (space group *C*2/*c*) [3], while the pink-colored $MnC_2O_4{\cdot}3H_2O$ is orthorhombic (space group *Pcaa* [4]). It is expected that the difference in the crystal lattice of the compounds and the different way of bonding of water molecules would affect some properties, such as a thermal stability, oxidation, and magnetic behavior.

While the reports on the thermal decomposition of manganese(II) oxalate trihydrate are quite scarce [5], this process is extensively studied in the case of $MnC_2O_4{\cdot}2H_2O$ in air atmosphere [6–19]. In addition to DTA and TG, other methods, such as gas analysis [6–9], isothermal annealing [6,8–10], solid-phase IR spectroscopy [8,9], and measurement of the electrical properties of the system [10], have been also applied. The reported results differ in the product types: MnO [11], mixture of MnO and Mn_3O_4 [12], Mn_2O_3 [6,7,13,14], $3MnO_2{\cdot}Mn_2O_3$, transforming immediately into $Mn_3O_4{\cdot}2MnO_2$ [15]. Mn_3O_4 is obtained either directly [16,17], or through the intermediate: mixture of MnO and MnC_2O_4 [10], Mn_5O_8 ($3MnO_2{\cdot}2MnO$ or $Mn_2^{II}Mn_3^{IV}O_8$) [9] or $MnCO_3$ [8]. The results depend on the environment (static, dynamic, self-generated), sample quantity and parti-

* Corresponding author. Tel.: +359-2-8161215; fax: +359-2-9625438.
E-mail addresses: nhbd@inorg.chem.uni-sofia.bg (B. Donkova), metkomeh@svr.igic.bas.bg (D. Mehandjiev).
[1] Tel.: +359-2-8703254; fax: +359-2-8705024.

0040-6031/$ – see front matter © 2004 Elsevier B.V. All rights reserved.
doi:10.1016/j.tca.2004.04.001

cle size, annealing rate and duration, shape of the TG container, etc. [18]. In the present case, the system is extremely complex due to the existence of a great number of simple and mixed stoichiometric manganese oxides, the possibility of formation of non-stoichiometric oxide systems, as well as the occurrence of secondary gas–gas and gas–solid processes caused by the evolution of H_2O, CO, and CO_2.

However, at least one more factor should be added to the aforementioned ones, namely the effect of the preparation conditions on the type and structure of the initial specimen. It has been established that the obtaining of a pure phase of α-$MnC_2O_4{\cdot}2H_2O$ by spontaneous crystallization strongly depends on pH [4], on the nucleation mechanism (i.e., the temperature and concentration), and on the contact time with the mother liquor (Donkova and Djarova, submitted for publication). Depending on the synthetic path, the specimens of the formula $MnC_2O_4{\cdot}2H_2O$ subjected to thermal analysis in the literature cited could be pure monoclinic dihydrate, partially dehydrated at 100 °C orthorhombic trihydrate, or a mixture of them.

The aim of the present work is to study the effect of the starting crystal lattice of the crystallohydrate on the mechanism of decomposition and the type of the products obtained by investigation and comparison of the processes of thermal decomposition of α-$MnC_2O_4{\cdot}2H_2O$ and $MnC_2O_4{\cdot}3H_2O$, using in situ measurements of their magnetic properties. This method allows the direct determination of the oxidation state of the Mn^{n+} ions and their coordination during the decomposition process. Additional information was obtained by means of thermal analysis, as well as by X-ray diffraction.

The only comparison between the dihydrate and the trihydrate, found so far, concerns only their thermal dehydration and the structure of the anhydrous oxalate [4]. A study of the thermal decomposition processes by measuring the magnetic properties of the aforementioned objects has not been found so far in the literature.

2. Experimental

2.1. Synthesis of $MnC_2O_4{\cdot}2H_2O$ and $MnC_2O_4{\cdot}3H_2O$

Samples of $MnC_2O_4{\cdot}2H_2O$ and $MnC_2O_4{\cdot}3H_2O$ were obtained by spontaneous crystallization. The initial reagents were "high purity" grade $MnCl_2{\cdot}4H_2O$ and $K_2C_2O_4{\cdot}H_2O$. The preparation conditions were $T = 25$ °C, controlled acidity of the medium (pH $= 3.0 \pm 0.1$), and continuous stirring of the reaction system.

The type of crystallohydrate obtained depends on the nucleation mechanism—homogeneous for $MnC_2O_4{\cdot}2H_2O$ and heterogeneous for $MnC_2O_4{\cdot}3H_2O$. This fact determines the different concentrations of the initial solutions. The synthesis of $MnC_2O_4{\cdot}2H_2O$ was carried out for 24 h and the obtained white precipitate was filtered, washed with bidistilled water, and air dried. The synthesis of the pink-colored $MnC_2O_4{\cdot}3H_2O$ took place for 40 min and, after filtration and washing, the product was dried in a vacuum desiccator on silica gel.

2.2. Synthesis of manganese oxides—MnO_x

For the comparison of the isothermal behavior of the two crystallohydrates, three samples were taken from each of the two initial oxalates. Each sample was annealed for 1 h in air atmosphere at 300, 400, and 450 °C. The samples were then tempered in a desiccator and weighed. Six samples prepared in this way are denoted as MnO_x in the text.

2.3. Characterization and investigation

The obtained crystallohydrates—α-$MnC_2O_4{\cdot}2H_2O$ and $MnC_2O_4{\cdot}3H_2O$, as well as the oxides obtained from them—MnO_x, were investigated by the following methods:

2.3.1. Thermal analysis

The thermal investigations were performed on a Paulik-Erdey MOM OD-102 derivatograph. The DTA and TG curves were obtained in a static air atmosphere with sample mass of 0.200 g at a heating rate of 10 °C/min in the 25–550 °C temperature range, using a standard corundum crucible. The reference sample was pure α-Al_2O_3. DSC analysis was carried out in a dynamic air atmosphere on Mettler TA3000 and DSC 20 apparatuses at a heating rate of 20 °C/min.

2.3.2. X-ray diffraction analysis

The XRD analysis was carried out with a D 500 Siemens powder diffractometer using Cu Kα radiation in a 2θ diffraction interval of 10–60°. The stepwise scanning was performed with a 0.02° 2θ step and counting time of 2 s per step. The identification of the phases was realized by means of the database JCPDS—International Centre for Diffraction Data.

2.3.3. Magnetic measurements

The specific magnetic susceptibility of the two crystallohydrate forms, as well as that of the oxides obtained from them, was studied in the 25–300 °C temperature range (298–573 K) with a Faraday type magnetic balance. The respective weight losses (WL) were also determined. In the course of the in situ monitoring of the process of decomposition, the magnetic measurement was carried out by a stepwise increase of the temperature. At each step, the temperature was kept constant for 30 min before starting the measurements.

The effective magnetic moments of the samples MnO_x were calculated on the basis of the Curie–Weiss law, using the values of the magnetic susceptibilities.

In the case of in situ measurements, the magnetic moments were calculated as:

$$\mu_{\text{eff}} = 2.828[\chi(T - \theta)]^{1/2}$$

where μ_{eff} is the effective magnetic moment in Bohr's magneton BM; χ is the molar magnetic susceptibility; T is the absolute temperature in K; θ is the Weiss constant in K. While the magnetic moment enables the determination of the oxidation state of the metal, the Weiss constant depends on the environment of the given ion and it is used to monitor changes in the character of interaction between the metal ions [20–23].

3. Results

3.1. Thermal analysis

This study was carried out in order to obtain preliminary information about the thermal behavior of α-$MnC_2O_4{\cdot}2H_2O$ and $MnC_2O_4{\cdot}3H_2O$. The results are represented in Figs. 1 and 2. In the case of the monoclinic $MnC_2O_4{\cdot}2H_2O$, the dehydration starts at about 130 °C and proceeds in one step (peak at 175 °C). The experimentally determined weight loss of 20% is in agreement with the calculated value. In the case of the orthorhombic $MnC_2O_4{\cdot}3H_2O$, the dehydration starts at a lower temperature of ≈80 °C and ceases at ≈210 °C. This is a three-step process (peaks at 120, 145, and 190 °C), which proves the different modes of binding of the water molecules. The experimental weight loss of 26.5% is lower than the theoretical one of 27.8%, this deviation being within the limits of the method accuracy. However, the slope in the trend of the TG curve suggests that, more probably, dehydration has not been fully completed.

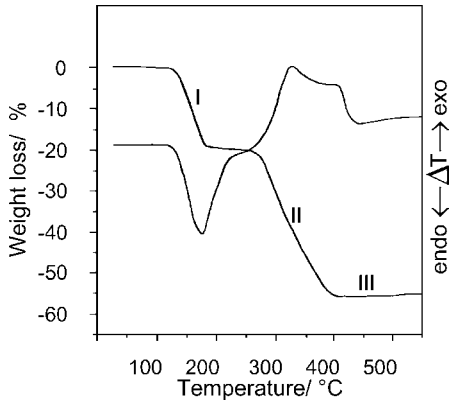

Fig. 1. DTA and TG curves of $MnC_2O_4{\cdot}2H_2O$.

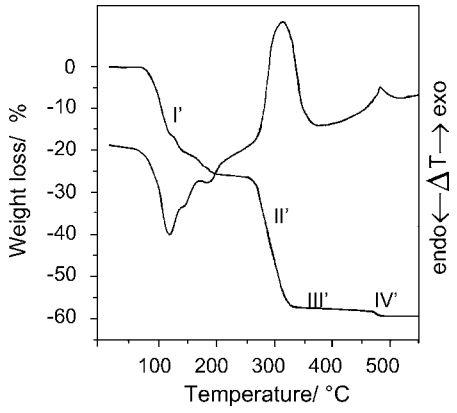

Fig. 2. DTA and TG curves of $MnC_2O_4{\cdot}3H_2O$.

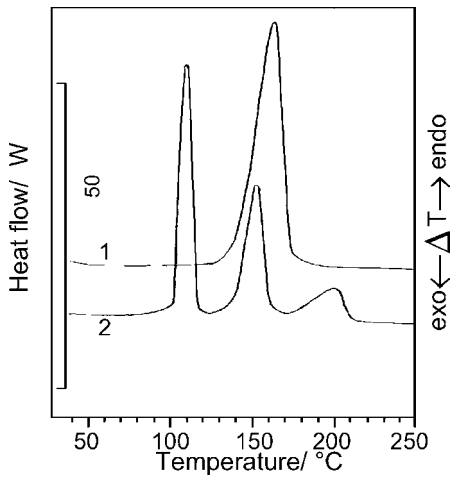

Fig. 3. DSC curves of $MnC_2O_4{\cdot}2H_2O$ (1) and $MnC_2O_4{\cdot}3H_2O$ (2).

In order to obtain additional information, the heat of dehydration of $MnC_2O_4{\cdot}2H_2O$ and $MnC_2O_4{\cdot}3H_2O$ were established by measuring the heat capacity. Fig. 3 shows the DSC curves, which reproduce quite well the trend of the DTA curves. The range of dehydration of $MnC_2O_4{\cdot}2H_2O$ is from 121 to about 195 °C, with a peak at 160 °C. The determined enthalpy of dehydration amounts to 97 kJ/mol, the respective literature value being 86 kJ/mol [24].

In the case of $MnC_2O_4{\cdot}3H_2O$, the range of the stepwise dehydration is 75–215 °C, with peaks at 109, 150, and 200 °C. These well defined peaks allow the exact determination of the bond energy for each water molecule. The respective values are $\Delta H_I = 59$ kJ/mol, $\Delta H_{II} = 45$ kJ/mol, and $\Delta H_{III} = 16$ kJ/mol. For the entire dehydration process $\Delta H = 132$ kJ/mol; a respective literature value was not found.

The trends of the DTA curves in Figs. 1 and 2 suggest that a difference exists also in the processes of decomposition and oxidation, taking place above ≈250 °C. For $MnC_2O_4{\cdot}2H_2O$, they result in two exothermal peaks at 330 and 400 °C, while for $MnC_2O_4{\cdot}3H_2O$ only one exo-peak at 303 °C is observed. An obvious difference between the two samples is the observation of an exo-peak at 480 °C in the DTA curve of $MnC_2O_4{\cdot}3H_2O$. The experimentally determined weight loss in region II of Fig. 1 is 55.5%, the respective theoretical values being 51.4% (MnO_2), 55.9% (Mn_2O_3), 57.38% (Mn_3O_4), and 60.35% (MnO). The analogous region for the trihydrate (region II′ in Fig. 2) has an experimental weight loss of 56.9%, the theoretical ones being 55.85% (MnO_2), 59.92% (Mn_2O_3), 61.27% (Mn_3O_4), and 63.97% (MnO). However, the process is obviously incomplete and passes through intermediate non-stoichiometric phases, since in the next region III′, the TG curve for the trihydrate shows a

"stable" decrease in the weight from 56.9 to 58.46%. The weight loss in region IV′ is 59.23%.

The products obtained by the thermal decompositions are not defined from the TG curves, since this is quite questionable in the case of such complex systems as the oxalates of the d-elements. The reasons for this are well grounded in [25]. The data obtained from the thermal analysis show only the changes occurring in the process of decomposition and reveal the differences in the two crystallohydrates. As seen in Fig. 3, the initial temperature of dehydration of the dihydrate is the same as that for the separation of the second water molecule in the trihydrate, but the final dehydration temperature is different in the latter case. This in turn shifts the region of existence of the anhydrous oxalate. On the other hand, the enthalpy of dehydration of $MnC_2O_4{\cdot}2H_2O$ is compared with the activation energy in [26], and a conclusion is drawn concerning the composition of the intermediate complex. It should be taken into account that ΔH of the second and third water molecule in the trihydrate (66 kJ/mol) is close to the reported activation energy value for the dihydrate, but it reflects relations of completely different nature.

3.2. X-ray diffraction analysis

The XRD patterns of $MnC_2O_4{\cdot}2H_2O$ and $MnC_2O_4{\cdot}3H_2O$ coincide complete those of the reference compounds. The monoclinic $MnC_2O_4{\cdot}2H_2O$ was identified according to card JCPDS No. 25-0544 and the orthorhombic $MnC_2O_4{\cdot}3H_2O$—according to card JCPDS No. 32-0648.

The X-ray patterns of the obtained after annealing manganese oxides MnO_x are represented in Figs. 4 and 5 as dash diagrams in order to visualize and compare the obtained phases. The dash diagrams of Mn_3O_4 (JCPDS No. 24-0734) and Mn_2O_3 (JCPDS No. 41-1442) are given as references in the same figures.

In the case of initial $MnC_2O_4{\cdot}2H_2O$, at 300 °C the sample is still strongly amorphous and the most intensive reflections in the crystallizing phase are those of Mn_3O_4. The weight loss of 54% shows that annealing for 1 h at 300 °C is insufficient for the completion of the oxidative decomposition and that the process is in region II of the TG curve in Fig. 1. The presence of MnO_2 (WL 51.4%) is possible, together with Mn_2O_3 (WL 55.9%) and Mn_3O_4 (WL 57.4%). At 400 °C (WL 56.5%), the predominant phase is Mn_3O_4, although the strongest line of Mn_2O_3 emerges, too. At 450 °C, there is already a complete transformation into hausmannite, Mn_3O_4 (full coincidence with the reference material No. 24-0734, shown in the same figure), which is confirmed by the experimental weight loss of 56.96% (theoretical value of 57.4%). In the DTA experiments, such a complete transformation is observed only at 960 °C.

The literature data for the isothermal annealing of the dihydrate are as follows. Mn_3O_4, has been obtained after annealing at 300 °C for 1 h in [8], at 350 °C, this has been the only phase and a coincidence with JSPDS No. 24-0734 is reported. In [10] at 340 and 400 °C, Mn_3O_4, has been predominantly obtained but the annealing time is not indicated. After annealing at 300 °C for 5 h, the obtaining of slightly crystalline Mn_5O_8 and small amounts of Mn_3O_4 is reported in [9]; Mn_3O_4 is reported to be the main phase after annealing for the same time, but at 600 °C. Consequently, in the temperature range 300–600 °C, the type of the oxide obtained depends on both the temperature and the annealing duration. A detailed analysis of the influence of these factors on the product types is given in [6]. Depending on the annealing time, different final products can be obtained at the same temperature. The results, however, follow the trend in the thermodynamic stability of the oxides Mn(IV) → Mn(III) → Mn(III) + Mn(II) [27] and the transitions, established with these systems [28].

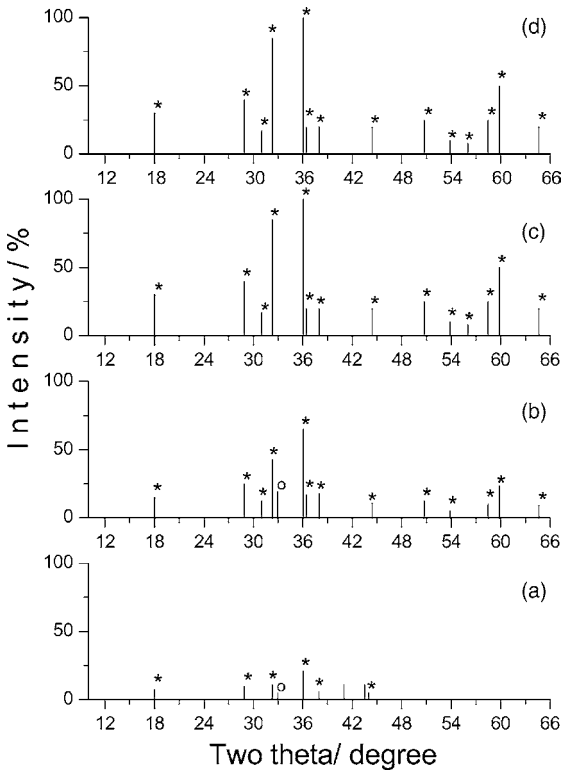

Fig. 4. Dash-diagrams of the three MnO_x samples, obtained after annealing of $MnC_2O_4{\cdot}2H_2O$ (a) at 300 °C; (b) at 400 °C; (c) at 450 °C; (d) Mn_3O_4—JCPDS 24-0734. *Legend*: (*) Mn_3O_4; (°) Mn_2O_3.

From this point of view, the results obtained starting with the trihydrate (Fig. 5) are more interesting and they confirm that the difference between the two crystallohydrates is not only in the different release of water. When the initial substance is $MnC_2O_4{\cdot}3H_2O$ at 300 °C, the sample is less amorphous, which explains the stronger intensity of the peaks and facilitates their identification. The only crystallized phase observed is Mn_3O_4. At 450 °C, the difference between the phases obtained from the two initial manganese crystallohydrates is obvious. In this case, two phases are observed in the sample—Mn_3O_4 and Mn_2O_3. The experimentally determined weight losses are 59.14% (300 °C), 59.5% (400 °C), and 60.9% (450 °C), the calculated ones being

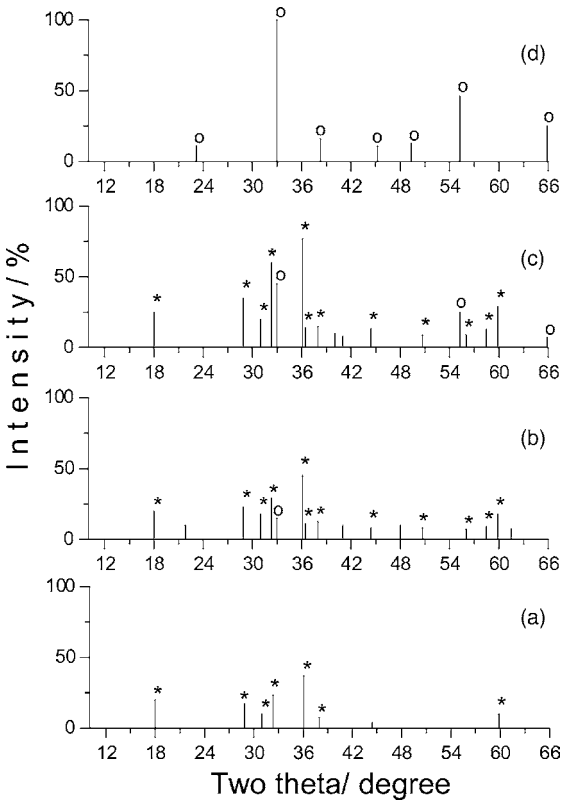

Fig. 5. Dash-diagrams of the three MnO_x samples, obtained after annealing of $MnC_2O_4{\cdot}3H_2O$ (a) at 300 °C; (b) at 400 °C; (c) at 450 °C; (d) Mn_2O_3—JCPDS 41-1442. *Legend*: (*) Mn_3O_4; (°) Mn_2O_3.

55.85% (MnO_2), 59.9% (Mn_2O_3), and 61.27% (Mn_3O_4). Regardless of close experimental weight loss values the diffractograms in Fig. 5 show that the residues obtained differ in composition and prove that the definition of the DTA product based solely on the weight losses is quite questionable and the transitions are interrelated.

3.3. Magnetic measurements

3.3.1. Magnetic susceptibility

Figs. 6 and 7 represent the temperature dependences of the specific magnetic susceptibility (χ_s) of both initial samples of manganese(II) oxalates, as well as those of the obtained manganese oxides MnO_x in the temperature range of 25–300 °C. The decrease in χ_s with the increase of temperature shows that all the samples studied display paramagnetic properties.

3.3.2. Magnetic moments

As it was already pointed out, the calculation of the magnetic moments provides information about the changes in the oxidation state of the Mn^{n+} ions during thermal decomposition. The magnetic moments μ_{eff} of the samples studied were calculated from the magnetic susceptibility using the Curie–Weiss law. The values obtained for μ_{eff}, represented in Table 1, were calculated within the range of 25–80 °C for

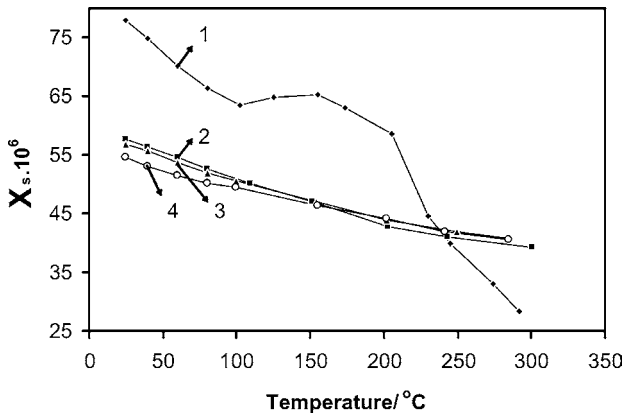

Fig. 6. Temperature dependences (25–300 °C) of the specific magnetic susceptibility of $MnC_2O_4{\cdot}2H_2O$ (curve 1) and MnO_x samples obtained after annealing at 300 °C (curve 2), 400 °C (curve 3), and 450 °C (curve 4).

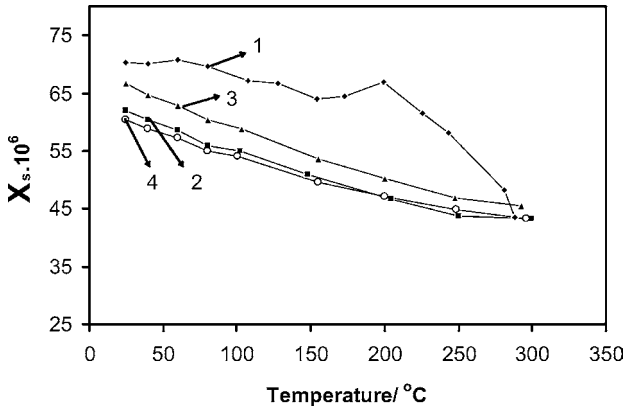

Fig. 7. Temperature dependences (25–300 °C) of the specific magnetic susceptibility of $MnC_2O_4{\cdot}3H_2O$ (curve 1) and MnO_x samples obtained after annealing at 300 °C (curve 2), 400 °C (curve 3), and 450 °C (curve 4).

the initial $MnC_2O_4{\cdot}2H_2O$ and $MnC_2O_4{\cdot}3H_2O$ and within 25–300 °C for the oxides. The values of the Weiss constant, θ, are given in the same table, as well as the correlation coefficients, R. The values R show that the law is valid with a high degree of reliability. The negative values of the constant of Weiss indicate that all samples are antiferromagnetic, the

Table 1
Effective magnetic moments of $MnC_2O_4{\cdot}2H_2O$ and $MnC_2O_4{\cdot}3H_2O$ (in the range of 25–80 °C) and of the oxides (in the range of 25–300 °C), prepared by isothermal annealing

No.	Sample	μ_{eff} (BM)	θ (K)	R
1	$MnC_2O_4{\cdot}2H_2O$	5.92	−13	0.999
2	MnO_x (from $MnC_2O_4{\cdot}2H_2O$) 300 °C	4.44	−259	0.9972
3	MnO_x (from $MnC_2O_4{\cdot}2H_2O$) 400 °C	4.75	−351	0.9983
4	MnO_x (from $MnC_2O_4{\cdot}2H_2O$) 450 °C	5.07	−474	0.9985
5	$MnC_2O_4{\cdot}3H_2O$	5.92	−13	0.999
6	MnO_x (from $MnC_2O_4{\cdot}3H_2O$) 300 °C	4.75	−299	0.9939
7	MnO_x (from $MnC_2O_4{\cdot}3H_2O$) 400 °C	4.79	−266	0.9981
8	MnO_x (from $MnC_2O_4{\cdot}3H_2O$) 450 °C	5.02	−387	0.9975

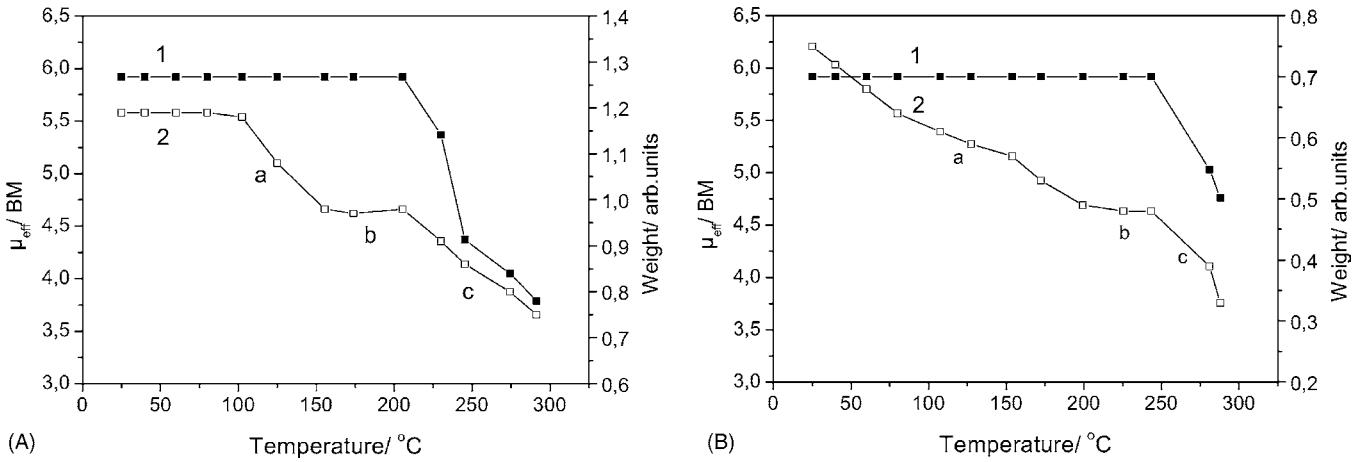

Fig. 8. Temperature dependence of the magnetic moments (curve 1) and the weight during in situ magnetic measurements (curve 2) of (A) $MnC_2O_4{\cdot}2H_2O$ and (B) $MnC_2O_4{\cdot}3H_2O$.

temperature of Neel being lower than 25 °C. The lower absolute θ values in the initial oxalates indicate weaker antiferromagnetic interaction in these samples. The higher $|\theta|$ values in the oxides are an indication of stronger antiferromagnetic exchange interaction.

3.4. Changes in the magnetic moments of $MnC_2O_4{\cdot}2H_2O$ and $MnC_2O_4{\cdot}3H_2O$ upon dehydration and decomposition

The magnetic moments of the initial oxalates at a given temperature are shown as curves 1 in Fig. 8A and B. The results are compared with the weight losses of the samples of $MnC_2O_4{\cdot}2H_2O$ and $MnC_2O_4{\cdot}3H_2O$ versus temperature (curves 2 in Fig. 8A and B) during in situ magnetic measurements. The regions denoted on the TG curves basically correspond to the following processes: (a) dehydration of $MnC_2O_4{\cdot}2H_2O$ and $MnC_2O_4{\cdot}3H_2O$, respectively; (b) region of existence of anhydrous oxalates; (c) decomposition of the oxalates.

4. Discussion

The value of the manganese magnetic moment depends on its oxidation state, its coordination state, and the strength of the crystal field [20–22]. In the case of the oxalate ions, it should be expected that the crystal field is of an intermediate strength and the values of μ_{eff} for the various oxidation states are 5.92 BM for Mn(II), 4.70 BM for Mn(III), and 3.44 BM for Mn(IV) [21]. The value of the magnetic moment, calculated for the initial oxalates (Table 1, samples 1 and 5) fully coincides with the theoretically expected value of 5.92 BM, which means that manganese is in the (+2) oxidation state.

The TG curves of the initial oxalates (curves 2 in Fig. 8A and B) demonstrate both the different mode of binding of the water in crystal lattice and the temperature differences upon decomposition. An interesting fact is that the temperature dependences of the magnetic moments of the two crystallohydrates $MnC_2O_4{\cdot}2H_2O$ and $MnC_2O_4{\cdot}3H_2O$ are also different (curves 1 in Fig. 8A and B).

The dehydration of $MnC_2O_4{\cdot}2H_2O$ proceeds in region **a** in Fig. 8A. Since the oxidation state of manganese(II) is being preserved during the entire dehydration process, it follows that the magnetic moment should not change. Indeed, μ_{eff} remains constant in this temperature range, which is an indication that there is only Mn(II) in the sample.

In the case of $MnC_2O_4{\cdot}3H_2O$, dehydration occurs with a stepwise decrease of the weight (region **a** in Fig. 8B). If one assumes that θ has a constant value or equals zero, then the calculated magnetic moment μ_{eff} shows an unexpected increase in its value upon dehydration of the sample. However, there is no noticeable change in the oxidation state, in the coordination state, or in the field strength, since this would lead to a decrease not to an increase in the magnetic moment of Mn(II). Therefore, one should suppose that θ is changing upon dehydration of this sample, while the oxidation state is being preserved, i.e., μ_{eff} remains constant.

Fig. 9 represents the temperature dependences of the constant θ for the two crystallohydrates calculated at μ_{eff} =

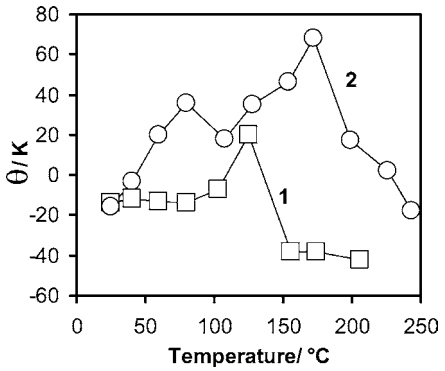

Fig. 9. Temperature dependence of the Weiss constant, θ, for $MnC_2O_4{\cdot}2H_2O$ (curve 1) and $MnC_2O_4{\cdot}3H_2O$ (curve 2) calculated at μ_{eff} = 5.92 BM.

5.92, corresponding to the existence of Mn(II)-ions. The constant of Weiss depends on the number of neighbors, with which the respective ions are interacting, and also on the sign of the exchange integral [23]. While in the case of $MnC_2O_4{\cdot}2H_2O$ (curve 1), the negative value of θ is preserved almost within the entire temperature range, a change in the sign is observed for $MnC_2O_4{\cdot}3H_2O$ (curve 2) from the very beginning of the dehydration process. This observation shows that upon dehydration of $MnC_2O_4{\cdot}3H_2O$ the indirect exchange between the Mn(II) ions changes from antiferromagnetic into a ferromagnetic one. At the end of the process, θ acquires again a negative value, which is an evidence of antiferromagnetic interaction.

The regions denoted by **b** in Fig. 8A and B represent the temperature ranges of existence of the anhydrous oxalates, and they are different for the two crystallohydrates. When the initial material is monoclinic α-$MnC_2O_4{\cdot}2H_2O$, the anhydrous oxalate is stable at lower temperatures. The absence of considerable changes in the TG curves for both samples shows that there are no transformations, occurring within this temperature range. This fact allows us to assume that the oxidation state, respectively the magnetic moment μ_{eff}, is preserved almost constant (curves 1, Fig. 8A and B), while θ is varying due to the change in the nature of the exchange interaction.

The oxidative decomposition of the anhydrous oxalates proceeds in the regions **c** in Fig. 8A and B. For the two samples, however, the initial temperatures of this process are different. In the case of $MnC_2O_4{\cdot}2H_2O$, the respective value is $T \geq 205\,^{\circ}C$, while for $MnC_2O_4{\cdot}3H_2O$ T is $\geq$243.5 °C. The values, obtained for μ_{eff} (curves 1 in Fig. 8A and B), are an indication that the mechanism of this oxidation depends on the initial crystallohydrate form. In order to preserve the value of 5.92 BM for the magnetic moment (characteristic of Mn^{2+}) at these two temperatures, the absolute value of the constant of Weiss should be very high $|\theta| \approx 610$, which is impossible. This is an evidence of the occurrence of oxidation processes. However, it should be noted that: (i) the decrease in the magnetic moments is much stronger than expected, if one assumes that the oxidation proceeds only to the formation of Mn_3O_4 (for the pure hausmanite $\mu_{eff} =$ 5.14 BM) and (ii) the magnetic moments of the two oxalates decrease to a different extent.

In the in situ investigations, the oxidation process with the initial $MnC_2O_4{\cdot}2H_2O$ leads essentially to Mn(IV), as indicated by the obtained μ_{eff}, which is closer to the theoretical value for Mn(IV) than to that for Mn(III). The respective μ_{eff} in the case of initial $MnC_2O_4{\cdot}3H_2O$ indicates that at the same temperature the oxidation process is less intensive.

These results are confirmed also by the values of μ_{eff} for the MnO_x obtained after isothermal annealing at 300 °C (Table 1, samples 2 and 6). Again, the calculated μ_{eff} for both samples are considerably lower than 5.14 BM and the value for sample 2 is lower than that for sample 6. Irrespective of the XRD data, suggesting that the crystal phase emerging in both samples is Mn_3O_4 (which is in agreement with literature data, see Section 3.2), the substantially lower μ_{eff} value is an indication of the presence of a great amount of Mn(IV) and Mn(III) species in an amorphous state. For this reason, as reported in [9], a slightly crystalline $2MnO{\cdot}3MnO_2$ together with traces of an Mn_3O_4-like phase is obtained only after annealing for 5 h of $MnC_2O_4{\cdot}2H_2O$ since the time period is necessary for the reorganization and crystallization of the Mn(II) and Mn(IV) species. The obtaining of $3MnO_2{\cdot}Mn_2O_3$, transforming immediately into $Mn_3O_4{\cdot}2MnO_2$, is reported in [15]. In [10], by studying the change in the electrical properties of $MnC_2O_4{\cdot}2H_2O$, it is reported that the conductivity characteristic of Mn_3O_4 cannot be achieved at about 300 °C, regardless of the fact that XRD data confirm its formation. In our opinion, the presence of higher oxidation states as well is the most probable explanation of the increase in electroconductivity at $T > 226\,^{\circ}C$ observed in [10].

The comparison of the samples obtained at 300 °C and the other oxides in Table 1 shows that μ_{eff} is raising with the increase in annealing temperature. It is seen, however, that this increase in the magnetic moment is much stronger in the specimens obtained from $MnC_2O_4{\cdot}2H_2O$. The obtained μ_{eff} values are in agreement with the phases established in the XRD analysis.

Based on the values of the magnetic moments of the oxides obtained after annealing of the two crystallohydrates (Table 1), one can determine the approximate content of Mn(IV) in the samples (Table 2).

Table 2
Mn(IV) content in the MnO_x samples obtained after annealing

Annealing temperature (°C)	Manganese(IV) (%) in the MnO_x	
	From $MnC_2O_4{\cdot}2H_2O$	From $MnC_2O_4{\cdot}3H_2O$
300	87	50
400	50	45
450	9	16

The differences in the starting temperatures of decomposition of the obtained anhydrous oxalates and the different rates of decrease in their magnetic moments are associated with the crystalline structure of the initial oxalates; it affects the different ways of dehydration and different texture, and probably the structure of the anhydrous product.

Dollimore ascertained that upon dehydration and during decomposition, or just before decomposition, 3d-oxalates undergo a strong increase in their surface area. This increase and the changes in the physical texture depend on numerous factors, such as shape and size of the initial particles, the compactness and the adhesion between particles, the ratio between the densities of the oxalate and of the solid product, as well as on whether the gases formed are removed as quickly as possible [17,18]. The investigated crystallohydrates differ in shape. Scanning electron microscopic observations were carried out in the present work. It was established that the monoclinic $MnC_2O_4{\cdot}2H_2O$ represents “rose-like” agglomerates with irregular arrange-

ment of their rounded "leaflets," while the orthorhombic $MnC_2O_4{\cdot}3H_2O$ is in the shape of long, smooth needles. The difference in the dispersities of the two crystallohydrates is obviously due to their mechanisms of nucleation, the latter being homogeneous for $MnC_2O_4{\cdot}2H_2O$ and heterogeneous for $MnC_2O_4{\cdot}3H_2O$ (Donkova and Djarova, submitted for publication). These facts could explained the different change of the surface area of the two products. An optical microscopic comparison of the product obtained after dehydration of the initial dihydrate and trihydrate is made in [4]. It shows that a powder is obtained in the first case, while in the second case the shape of the initial crystals is preserved. The our scanning electron microscopic observations established that the "leaflets" of the dihydrate breaking down during dehydration due to crack formation caused by the water release. The situation with the trihydrate is completely different. After dehydration, quite straight grooves are observed on the surface of the initial long smooth needles. Breakdown of these needles was not established.

Therefore, using monoclinic $MnC_2O_4{\cdot}2H_2O$ as the starting material, a considerably greater change in the surface and structure is established, which leads to amorphization of the sample, and which is not the case with the orthorhombic $MnC_2O_4{\cdot}3H_2O$. This determines the differences in the thermal and chemical stability of the obtained products and affects the kinetics of the thermal decomposition. The more developed surface possesses a greater reactivity, it is oxidized faster and to a greater extent, which explains the lower decomposition temperature of the product obtained from the dihydrate and the stronger decrease of its magnetic moment. According to literature data [7,13,29], in air atmosphere an oxidation process to Mn(III) takes place just before decomposition and calalyzes the later. After decomposition the evolved CO reduces Mn^{m+} to lower oxidation states and the present Mn^{m+} and Mn^{n+} catalyzes the oxidation of CO to CO_2 [29]. In the present work was established that the oxidation proceeds not only to Mn(III) but also to Mn(IV). For the above reasons, all redox processes are much more intensive when starting with $MnC_2O_4{\cdot}2H_2O$. Taking into account the necessity of crystallization of the obtained in this case amorphous phase, one can explain the more complex shape of the respective DTA curve.

The corresponding interval for $MnC_2O_4{\cdot}3H_2O$ is much narrower, proving comparatively limited oxy-reduction processes. In this case (1) the initial particles are considerable bigger, (2) the anhydrous oxalate has a higher degree of crystallization, and (3) the smaller change of the surface leads to a more weakly oxidized product and respectively to a slower decomposition process and a lower degree of reduction.

5. Conclusions

On the basis of the obtained magnetic data, it is proved that the oxidation of the anhydrous product leads not only to manganese(III) but also to manganese(IV), which is further pass to lower oxidation states. The oxidation processes proceeds to a different extent depending on whether the initial material is $MnC_2O_4{\cdot}2H_2O$ or $MnC_2O_4{\cdot}3H_2O$. This fact shows that the orthorhombic crystal lattice of the trihydrate stabilizes the lower oxidation states of manganese.

The annealing of the monoclinic α-$MnC_2O_4{\cdot}2H_2O$ at 450 °C leads to its complete transformation into tetragonal Mn_3O_4. At the same temperature, the orthorhombic $MnC_2O_4{\cdot}3H_2O$ gives not only Mn_3O_4, but also a large quantity of cubic Mn_2O_3.

Both crystallohydrates are paramagnetic. The exchange interaction between the manganese ions in $MnC_2O_4{\cdot}3H_2O$ is changing from antiferromagnetic to ferromagnetic during the entire dehydration process, while in the case of $MnC_2O_4{\cdot}2H_2O$ the same interaction remains almost constantly antiferromagnetic.

The enthalpy of dehydration of $MnC_2O_4{\cdot}3H_2O$ is determined to be 132 kJ/mol, the respective values for the first, second, and third molecule being 59, 45, and 16 kJ/mol.

References

[1] M. Gorgeu, Compt. Rend. 47 (1858) 929.
[2] Otto Hauser, F. Wirth, J. Pract. Chem. 79 (2) (1909) 358.
[3] R. Deyrieux, C. Berro, A. Peneloux, Bull. Soc. Chim. Fr. 1 (1973) 25.
[4] A. Huizing, H.A.M. van Hal, W. Kwestroo, C. Lahgereis, P.C. van Loosdregt, Mater. Res. Bull. 12 (1977) 605.
[5] K.B. Zaborenko, S.-C. Kung, L.L. Melikhov, V.A. Portyanoi, Radiokhimiya 6 (6) (1964) 749.
[6] D. Dollimore, J. Dollimore, J. Little, J. Chem. Soc. (A) (1969) 2946.
[7] M.E. Brown, D. Dollimore, A.K. Galway, J. Chem. Soc., Faraday Trans. 1 (70) (1974) 1316.
[8] A.K. Nohman, H.M. Ismail, G.A. Hussein, J. Anal. Appl. Pyrolysis 34 (1995) 265.
[9] M.I. Zaki, A.K. Nohman, Ch. Kappenstein, T.M. Wahdan, J. Mater. Chem. 5 (7) (1995) 1081.
[10] A.K. Nikumbh, A.E. Athare, S.K. Pardeshi, Thermochim. Acta 326 (1999) 187.
[11] C. Duval, Inorganic Thermogravimetric Analysis, Elsevier, Amsterdam, 1953.
[12] J. Robin, Bull. Soc. Chim. Fr. (1953) 1078.
[13] E.D. Macklein, J. Inorg. Nucl. Chem. 30 (1968) 2689.
[14] Gy. Baksy, A.J. Hegedus, Thermochim. Acta 10 (1974) 399.
[15] M.U. Jacob, D.D. Perlmutter, Thermochim. Acta 49 (1981) 207.
[16] D. Dollimore, D. Griffiths, D. Nicholson, J. Chem. Soc. 166 (1963) 2617.
[17] D. Dollimore, D. Nickolson, J. Chem. Soc. 165 (1962) 960.
[18] D. Dollimore, Thermochim. Acta 117 (1987) 331.
[19] D. Dollimore, J. Term. Anal. 11 (1977) 185.
[20] F.E. Mabbs, D.J. Machin, Magnetism and Transition Metal Complexes, Chapman and Hall, London, 1973, p. 153.
[21] D. Mehandjiev, S. Angelov, Magnetochemistry of Solid State, Nauka I Izkustvo, Sofia, 1979, p. 116.
[22] R. Boca, Theoretical Foundations of Molecular Magnetism, Elsevier, Amsterdam, Lousanne, New York, Oxford, Shannon, Singapore, Tokyo, 1999, p. 504.
[23] J.H. Van Vleck, J. Phys. 12 (1951) 262.

[24] K. Nagase, K. Sato, N. Tanaka, Bull. Chem. Soc. Jpn. 48 (2) (1975) 439.
[25] M. Maciejewski, E. Inger-Stocka, W.-D. Emmerich, A. Baiker, J. Therm. Anal. Cal. 60 (3) (2000) 735.
[26] D. Dollimore, N. Guindy, Thermochim. Acta 58 (1982) 191.
[27] D. Mehandjiev, R. Proiniva-Mehandjieva, Compt. Rend. Acad. Bulg. Sci. 33 (8) (1980) 1077.
[28] P. Pascal, Nouveau Traitè de Chimie Minerale, vol. XVI, 1960, pp. 748, 785.
[29] D. Dollimore, D.L. Griffiths, J. Therm. Anal. 2 (1970) 229.